An Improved Algorithm Based on SURF for MR Infant Brain Image Registration

Ke Du[1], Stéphane Domas[2], Michel Lenczner[1], Guangjin Zhang[3]

[1]FEMTO-ST Institute, Université de Technologie de Belfort-Montbéliard, France
{ke.du, michel.lenczner}@utbm.fr
[2]FEMTO-ST Institute, IUT Belfort-Montbéliard, France
stephane.domas@univ-fcomte.fr
[3]Hisense R & D center, Hisense Electric Co., Ltd. China
zhangguangjin@hisense.com

Abstract. The correct diagnosis of brain diseases is crucial for children with brain disorders. But the complex characteristics of infant brain make the image analysis very complicated. Thus, an accurate image registration is a prerequisite for accurate analysis of MR infant brain images, and it provides valuable information for the diagnosis of doctors. This paper presents our research works on SURF registration algorithm of 2-D MR infant brain images. We firstly describe the original algorithm and analyze its advantages and drawbacks. Then an improved version is proposed, which uses 8-D descriptor vectors with the length of 128. The experiment results show, compared to the original version, our algorithm can achieve more accurate image registration with a little more time consumption. For all the images tested, the increase of correct matching rate varies from a minimum of 5.7% to a maximum of 14.9% compared with the classical one.

Keywords: MR Image • SURF • Registration • Descriptor vector of features

1 Introduction

In recent years, the incidence of infant brain diseases is rising. Therefore, the correct diagnosis of infant brain diseases in early period has significance for children and it supposes a high quality analysis of the brain structure. For its complex characteristics, it usually requires manual analysis of doctors. Imaging processing technologies are widely used in medical applications. Nevertheless, to diagnose diseases from infant brain images is more difficult, it is a promising work.

In order to help doctors in this process, automatic comparisons could be done by a computer, so that it can bring original and valuable information for the diagnosis. The most important thing is to get low error rate. One solution is to use image registration, which is a very important technology in image processing. Its main purpose is to find similarity between two images and get the matching relationship of pixels. How to establish a reasonable correspondence between images is the key point. Until now, each image registration algorithm is restricted in one or several classes of images. None of them can be efficiently applied to all images. For MR infant brain image, the complexity makes it even more challenging.

In this paper, we describe our research works address the problem of images registration applied on 2-D MR infant brain images. The rest of this paper is organized as follows. Section 2 discusses related works including the background of image registration and necessity. In Section 3, we introduce the process of image registration based on descriptor vectors of interest points, especially SURF algorithm. An analysis of its advantages and drawbacks is provided. Section 4 elaborates on the improved SURF algorithm using an 8-D descriptor vector with the length of 128. Section 5 shows the experiment results. Finally, Section 6 gives the conclusions and outlooks.

2 Related Works

Image registration uses a number of similarity measure criteria to establish the relationship between two images, sample images and template image. Then, the parameters of the transformation models must be computed so that the corresponding relationship between pixels in two images can be found. At last, the registration result can be obtained [1, 2]. An example of images in registration is given in Fig. 1.

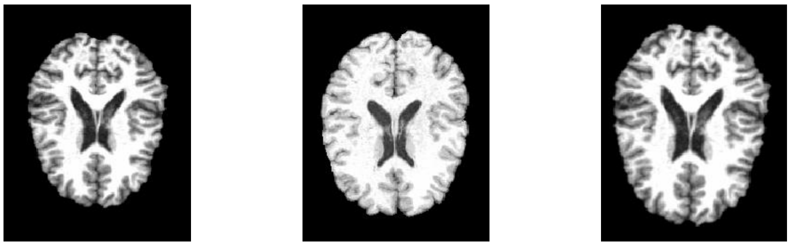

（a）Sample image （b）Template image （c）Registration result

Fig. 1. Schematic diagram of image registration

2-D image can be described as a two-dimensional matrix. $I_1(x, y)$ and $I_2(x, y)$ represent the grayscale of pixel $p(x, y)$ in sample image I_1 and template image I_2. The relationship between I_1 and I_2 can be defined as,

$$I_2(x, y) = g\left(f\left(I_1(x, y)\right)\right) \tag{1}$$

Where, f and g are geometric and grayscale transformation function respectively. Registration between images can be achieved by geometric transformation and grayscale transformation. Usually, the grayscale transform is not necessary in practice.

Generally, as shown in Fig. 2, the basic framework of image registration includes following steps [3,4]:

1. Input template image and sample image.
2. Image transformation to feature spaces.

3. Interpolation on grayscale and geometric transformation of sample image.
4. Computation of the similarity measure.
5. Optimization of the similarity measure to give the final transformation parameters.
6. Final interpolation of sample image according to transformation parameters.

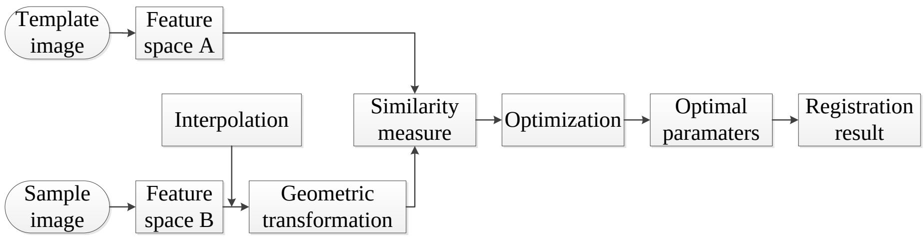

Fig. 2. Flow chat of image registration framework

There are a variety of image registration algorithms. Different ones are applied to different conditions. They can be divided into three categories, including grayscale-based algorithms, model-based algorithms and feature-based algorithms. The consumption of calculation of feature-based algorithms is much smaller than others', which leads to higher efficiency. Meanwhile, the algorithms have strong robustness regardless of the influence of illumination changes. The research works presented in this paper focus on obtaining even better performances with feature-based algorithms, by improving the accuracy in the context of 2-D MR infant brain images.

3 Image Registration Based on Features

Many researchers have carried out extensive researches proposed a number of widely used feature-based algorithms. They have a certain increase in either efferency or accuracy of matching. Among them, SIFT [5] was created by David Lowe and improved in 2004 [6]. It relies on a conversion from matching between two images to the similarity among descriptor vectors. The process of SIFT algorithm includes setup of multi-scale space, extracting interest points, getting descriptor vectors of features, and feature matching. It can handle changes in scale, translation and rotation. Since SIFT algorithm is fast and has so large numbers of applications in the field of image registration, currently, many researchers have put forward their improved SIFT version and achieved good results. In 2006, Bay H, Tuytelaars T and Van Gool L have proposed the SURF algorithm [7], which is faster and more robust. Although 2-D image registration algorithms based on features are a great achievement, due to the complex structure of brain, especially the infant brain, there are still improvements to find.

3.1 Multi-scale Space Setup

The basis of feature-based image registration algorithm is to extract interest points. There are many methods for interest point extraction, such as edge detection and Harris corner detection. However, due to the complex structure of infant brain image, methods used on natural images do not work very well. Therefore, in order to extract interest points, we need to set up multi-scale space of infant brain images. It is done by transformation to obtain images at different scales. For some image features can only be expressed in a particular scale, multi-scale space can be more effective to represent characteristics of images. Widely used multi-scale space is Gaussian multi-scale space [8]. It is defined by a Gaussian kernel function, as follows,

$$G(x, y, \sigma) = \frac{1}{2\pi\sigma^2} e^{-(x^2+y^2)/2\sigma^2} \tag{2}$$

For an image $I(x, y)$, its Gaussian multi-scale space can be described as,

$$L(x, y, \sigma) = G(x, y, \sigma) * I(x, y) \tag{3}$$

Where, x, y represent the horizontal and vertical coordinates of 2-D image. σ is the scale parameter, $L(x, y, \sigma)$ is the result in multi-scale space coordinate. The smoothness of the image can be set with σ, where a large value corresponds to a low resolution, on the contrary, a small value corresponds to a high resolution. In Gaussian multi-scale space, images in the same scale are results of convolution between Gaussian kernels of different sizes and original images. The images on different layers are produced by down-sampling from higher layers correspondingly. Thus, reasonable analysis and calculations can be done according to the image in different resolutions. Details of the image can be read at high resolutions, while the shape of different parts can be analyzed at low resolutions.

In order to extract interest points more effectively, Lowe proposed to approximate the Laplacian of Gaussians (LoG) by a Difference of Gaussians (DoG) filter [5].

For good performance, detector of interest points based on Hessian matrix is used. For a pixel $p(x, y)$ in a 2-D image $I(x, y)$, the Hessian matrix is defined as follows,

$$H(I(x, y)) = \begin{bmatrix} \frac{\partial^2 I}{\partial x^2} & \frac{\partial^2 I}{\partial x \partial y} \\ \frac{\partial^2 I}{\partial x \partial y} & \frac{\partial^2 I}{\partial y^2} \end{bmatrix} \tag{4}$$

Working with Gaussian detector done by Lindeberg [9], Hessian matrix takes the following form,

$$H(x, y, \sigma) = \begin{bmatrix} L_{xx}(x, y, \sigma) & L_{xy}(x, y, \sigma) \\ L_{xy}(x, y, \sigma) & L_{yy}(x, y, \sigma) \end{bmatrix} \tag{5}$$

Where, L_{xx}, L_{xy} and L_{yy} are convolutions between the image and second-order Gaussian partial derivatives, taking L_{xx} for an example, as follows,

$$L_{xx} = I(x, y) * \frac{\partial^2 G(x, y, \sigma)}{\partial x^2} \tag{6}$$

Although LOG approximation proposed by Lowe was a success, it has been further improved by Herbert in [10] with box filters. L_{xx}, L_{xy} and L_{yy} can be replaced by D_{xx}, D_{xy} and D_{yy}. And then, the Hessian matrix becomes the follow format,

$$H(x,y)=\begin{bmatrix} D_{xx} & D_{xy} \\ D_{xy} & D_{yy} \end{bmatrix} \tag{7}$$

Where, D_{xx}, D_{xy} and D_{yy} are convolutions between image and box filters.

These approximate second-order Gaussian derivatives can be evaluated at a very low computational cost with integral images. The calculation time therefore is independent of the filter size. The process shown in Fig. 3, from left to right, is the approximation of box filter for the Gaussian second order partial derivative in xy direction (L_{xy}). The grey regions are equal to zero.

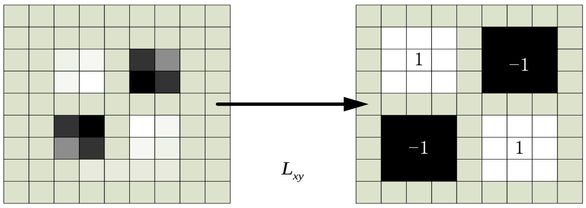

Fig. 3. Schematic diagram of box filter

For any pixel $p(x,y)$ in image $I(x,y)$, the integral image is denoted as,

$$I_{\Sigma}(x,y)=\sum_{i=0}^{i\le x}\sum_{j=0}^{j\le y} I(i,j) \tag{8}$$

The sum of intensities inside a rectangular region of any size can be calculated as,

$$S=D-B-C+A \tag{9}$$

Where, *A*, *B*, *C* and *D* represent the vertices of a rectangular region of an integral image as shown in Fig. 4. It takes only three additions and four memory accesses to calculate. Hence, the calculation time is independent of its size.

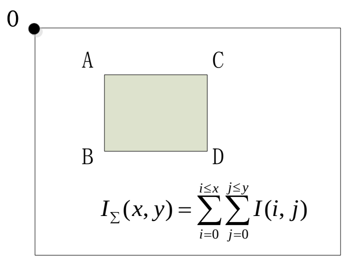

Fig. 4. Schematic diagram of integral image

Similar to Gaussian multi-scale space, the resolution of images goes down with σ becoming larger. Box filters with different sizes are used to make convolutions with images. Images at different resolutions constitute the box filter multi-scale space [11].

Interest point extraction is to extract significant changes in the image, which is one of the main steps in image registration based on features [12,13]. These points, working as matching points, can be either in image space or in scale-space, which include rich image information. Therefore, the quality of the extracted interest points impacts the registration results. In order to extract interest points in multi-scale space, we need to make comparisons between the target interest points and their neighbors. As shown in Fig. 5, the black point in the center is a target interest point, which should be compared with 26 points in its neighborhood.

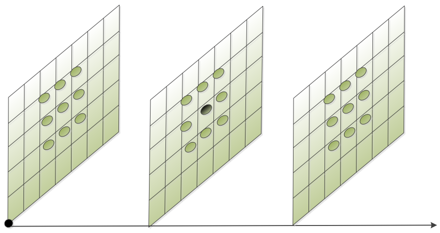

Fig. 5. Interest points extraction

Interest points are extracted from different scale spaces of the image but one comparison process uses only interest points of two scale spaces [14]. Thus, there are a portion of unstable interest points extracted from different scale spaces. In order to remove these unstable points, following derivation is necessary. The scale space function $D(x, y)$ is transformed with Taylor formula in *x*, and get the first three parts, as follows,

$$D(x,y) = D + \frac{\partial D^T}{\partial x} x + \frac{1}{2} x^T \frac{\partial^2 D}{\partial x^2} x \tag{10}$$

Let $D(x, y) = 0$, then,

$$\hat{x} = -\frac{\partial^2 D^{-1}}{\partial x^2} \bullet \frac{\partial D}{\partial x} \tag{11}$$

With a combination of equation (10) and (11), we can obtain,

$$D\left(\hat{x}, y\right) = D + \frac{1}{2} \frac{\partial D^T}{\partial x} \hat{x} \tag{12}$$

$|D(\hat{x}, y)|$ is used as a judgement, if $|D(\hat{x}, y)| \geq 0.03$, the interest point is stable and can be used to match the image. Usually, there are more interest points in high resolution image, which means more details. Conversely, in the low resolution image contains fewer details.

3.2 Interest Point Description

As the comparison in [15] shows, SURF is invariant to image scaling, blur, and illumination, and partially invariant to rotation and view point changes. Because 'Fast-Hessian' detector used in SURF is three times faster than DOG detector used in SIFT, SURF achieves better performances. However, SURF is not fully affine invariant. Therefore, Haar wavelet is used to detect the orientation [16].

An interest point should be selected in a circular neighborhood and calculate the sum of Haar wavelet responses within a sliding orientation sector window of 60°. Then, the window is rotated by a fixed angle, as shown in Fig. 6, and the sum is computed once again. After turning for a full circle, the direction with the maximum value is the orientation of the interest point.

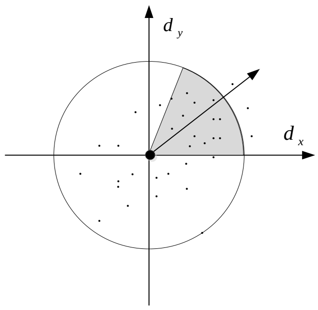

Fig. 6. Determination of orientation in SURF

After getting the orientation, it is possible to do the descriptor vector extraction. In SURF algorithm, a square region in the neighborhood of each interest point is chosen, and it is divided into 4×4 small squares, called sub-regions, as shown in Fig 7(a).

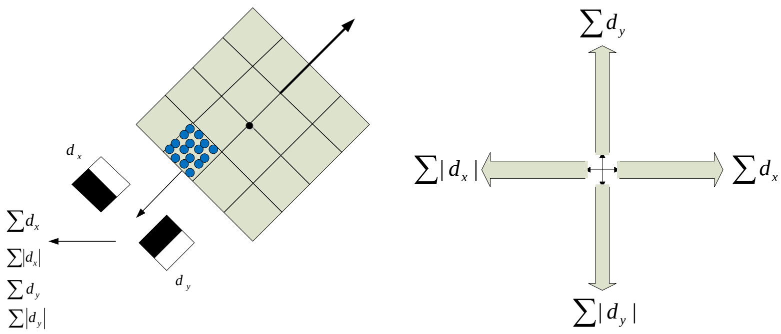

(a) Extraction of descriptor vector (b) 4-D descriptor vector of sub-region

Fig. 7. Descriptor vector of SURF algorithm

Then, the Haar wavelet responses are computed for each pixel in each sub-region. d_x and d_y represent the horizontal and vertical responses respectively, which are summed up as $\sum d_x$ and $\sum d_y$. In order to take intensity changes into consideration, the sum of the absolute values of the responses is calculated as $\sum|d_x|$ and $\sum|d_y|$. Thus, each sub-region has a 4-D descriptor vector, shown in Fig 7 (b). , written as,

$$v = (\sum d_x, \sum d_y, \sum|d_x|, \sum|d_y|) \tag{13}$$

In this way, we can obtain a 4-D descriptor vector with the length of 64 for the 4×4 sub-regions. And it can be used in the matching process. Descriptors obtained in this way are classical SURF descriptors [10].

3.3 Interest Point Matching

After getting the descriptor vectors of interest points, a matching between sample and template images can be done. Because of the nature of descriptor vector, the similarity measurement between vectors can be used. To make matching between interest points, we must take all the interest points in two images and calculate Euler distance between descriptor vectors. The shorter distance between two descriptor vectors means a higher degree of similarity, which represents the most similar interest points. Taking accuracy and consumption into account, we use the ratio of distance between the nearest neighbor and the second nearest neighbor to get the matching point.

For the interest point *A* in sample image *S* and the interest point *B* in template image *T*, the distance between the two descriptor vectors of *A* and *B* can be calculated by equation (14).

$$D_{AB} = \left[\sum_{l=0}^{l=m} (S_{Al} - T_{Bl})^2 \right]^{1/2} \tag{14}$$

Where, S_{Al} is the l_{th} descriptor vector of point *A*, T_{Bl} is the l_{th} descriptor vector of point *B*, and *m* is the number of the total dimensions of descriptor vectors. After calculating the distances between *A* and all the interest points of image *T*, we can get the nearest neighbor *N* and second nearest neighbor N'. A judgement is defined as,

$$\theta = D_{AN} / D_{AN'} \tag{15}$$

If θ is less than a certain threshold, *A* can be matched with *B*, else there is no matching point in image *T*. The number of matching points will increase with a larger threshold, and it will also increase the number of mismatching points. Thus, the threshold is usually 0.7. The principle of this method is relatively simple, a little time consuming, highly efficient and perfectly adapted to 2-D image matching.

4 Improved SURF Algorithm

SURF algorithm is a registration algorithm based on descriptor vectors of features proposed to improve SIFT algorithm. Compared with SIFT, it focuses on fast matching, and therefore improves the operating efficiency significantly. But the accuracy can be improved for some reasons. The interest points extracted by box filters are not real corners. There are large numbers of interest points on high resolution images including some unstable interest points, which will affect both the efficiency and accuracy. Each interest point is described as a 4-D descriptor vector with length of 64 for the 4×4 sub-regions. The less amount of computations lead to the high efficiency. The features can be described more accurately, especially for some high required applications. Our work is to improve it by increasing the dimensions of descriptor vectors. d_x and d_y can be regarded as the approximate differential of the image. $d_x > 0$ means the increasing trend in gray gradient of image in positive horizontal direction, while $d_x < 0$ means the decreasing trend. Thus, we express the 4-D descriptor vector in a new way as follows,

$$v = (\sum d_{0^\circ}, \sum d_{90^\circ}, \sum d_{180^\circ}, \sum d_{270^\circ}) \tag{16}$$

Which includes 4 directions $(0^\circ, 90^\circ, 180^\circ, 270^\circ)$ in the vector, shown in Fig. 8 (a).

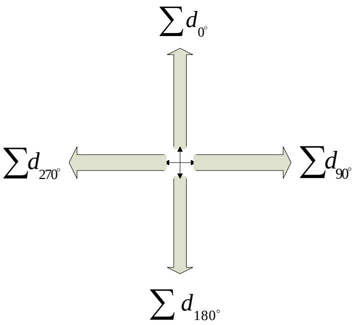

(a) The expressed 4-D descriptor vector

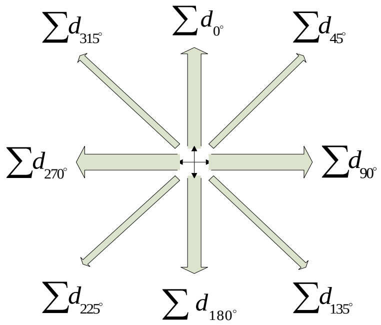

(b) The new 8-D descriptor vector

Fig. 8. The changing in descriptor vector of sub-region

In order to get more details of features in the descriptor vector, four other directions $(45^\circ, 135^\circ, 225^\circ, 315^\circ)$ are added to the vector. Thus, the new descriptor vector becomes an 8-D vector, shown in Fig.8 (b), written as,

$$v = (\sum d_{0^\circ}, \sum d_{45^\circ}, \sum d_{90^\circ}, \sum d_{135^\circ}, \sum d_{180^\circ}, \sum d_{225^\circ}, \sum d_{270^\circ}, \sum d_{315^\circ}) \tag{17}$$

The value of d_{45°, d_{135°, d_{225° and d_{315° can be calculated directly in the same way used as d_{0°, d_{90°, d_{180° and d_{270°. But it will leads to huge time consumption similar as the case of D-128 talked in [7]. Here an approximation is made as follows,

$$d_{45^\circ} = \sqrt{2}/2 d_{0^\circ} + \sqrt{2}/2 d_{90^\circ} \tag{18}$$

$$d_{135^\circ} = \sqrt{2}/2 d_{90^\circ} + \sqrt{2}/2 d_{180^\circ} \tag{19}$$

$$d_{225^\circ} = \sqrt{2}/2 d_{180^\circ} + \sqrt{2}/2 d_{270^\circ} \tag{20}$$

$$d_{315^\circ} = \sqrt{2}/2d_{270^\circ} + \sqrt{2}/2d_{0^\circ} \tag{21}$$

Consequently, the vector of a 4×4 region contains more detailed information of the image, and the length of which is 128. Actually, the approximation and extension of vector yields better matchings, as shown in experiment section. With the 8-D descriptor vector, the specific registration process can be operated in the following steps.

1. Build the multi-scale space of sample and template images with box filters of different sizes. Here, it includes three layers, and four images in each layer.
2. According to the Hessian matrix approximation, extract the interest points in the middle 10 images, and remove some unstable ones.
3. For each interest point extracted, according to Haar wavelet responses, can get the orientation of each interest point.
4. Calculate 8-D descriptor vectors in the neighborhood of 4×4 square sub-regions of the interest points in sub-regions with improved SURF algorithm.
5. Achieve the matching of two images with the ratio of distance between the nearest neighbor and the second nearest neighbor.

5 Experimental Results

In order to test the effect of the improved SURF algorithm, the experiment is carried out on a computer with CPU Intel Core i5 2.5GH and RAM 8.0GB, using Matlab2013b. 5 groups of images are tested. The first group is shown in Fig 9.

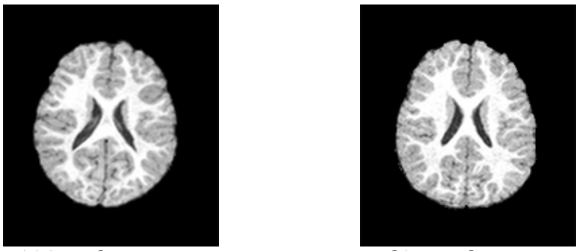

(a)Sample image (b)Template image

Fig. 9. Images being tested

The interest points are obtained with both the classical SURF algorithm and the improved SURF algorithm. The results of matching between interest points of sample images and template images correspondingly are shown in Fig. 10. In both image (a) and (b), 60 pairs of interest points are shown. In order to see visually whether they match correctly, colored links are used. It is obvious that there are more interest points matched correctly in the improved one.

Specific data, including numbers of points matched correctly (NC) and mismatching points (NM), correct matching rate (CR) and time consumption (T) are shown in Table. 1.

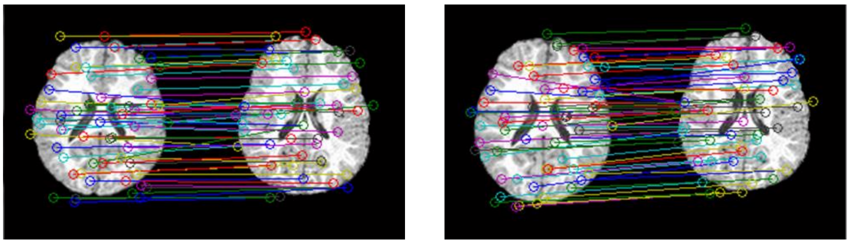

(a)Group 1 with classical SURF (b) Group 1 with improved SURF

Fig. 10. The results of interest points matching

Table 1. Comparison of interest point matching results

	NC	NM	CR/%	T/s
Classical SURF	52	8	86.7	1.112
Improved SURF	57	3	95.0	1.201

With the improved SURF, there are 57 out of 60 interest points matched correctly, 5 more than the classical SURF. The correct matching rate is 95.0% compared with the classical one with 86.7%. There are improvements obviously in the result. For the 8-D descriptor vectors with length 128, the time consumption of improved SURF is a little more, from 1.112s to 1.201s, increasing by 8.87%. But compared with the increasing in accuracy, the time consumption is acceptable. The results of image registration are shown in Fig. 11, where on the left is the result of classical one, the improved one is on the right and the template image is in the middle.

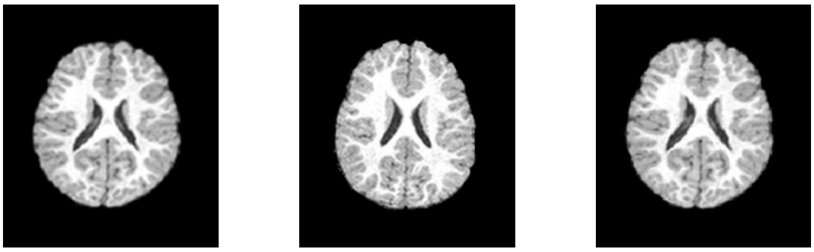

(a) Group 1 with classical SURF (b) Template image (c) Group 1 with improved SURF

Fig. 11. The results of image registration

To evaluate the similarity of the images, we make the segmentation according to the results of image registration. The results of segmentation are shown in Fig. 12, where the segmentation result according to classical SURF is on the left, the improved one is on the right and the template image is in the middle.

Jaccard similarity coefficient is defined as following,

$$J_{sc}\left(A,B\right)=\frac{\left|A\cap B\right|}{\left|A\cup B\right|} \tag{22}$$

Where, A and B represent the set of segmentation results according to template image and image registration result respectively. In this paper, the coefficient is used to evaluate the similarity between the two images. The higher the similarity is, the bigger the value is. In the ideal case, if the two sets are the same, the value should be 1, the maximum value. Different parts of brain in each group of images are chosen as the sets. The Jaccard similarity coefficient of all the groups can be found in Table 2. The result obtained by improved SURF is better than the classical one, where every parts of the brain have higher similarity to the template image for the higher value.

(a) Group 1 with classical SURF (b) Template image (c) Group 1 with improved SURF

Fig. 12. The results of image segmentation

To make it more convincing, the statistics of accuracy, similarity coefficient and time consumption for all groups of images are shown in Table 2. Generally, as for the higher accuracy, the improved SURF algorithm has better performance on the registration than the classical one. For all the images tested, the increase of correct matching rate varies from a minimum of 5.7% to a maximum of 14.9% compared with the classical one. The similarity coefficient is also increased in different degrees, which is consistent with the correct matching rate. The increase of time consumption varies from 5.28% to 19.6%, which is still acceptable compared to the gain for registration. Nevertheless, this point constitutes a problem to address in future works.

Table 2. Comparison of registration performance

	Classical SURF			Improved SURF		
No.	CR/%	J_{SC}	T/s	CR/%	J_{SC}	T/s
1	86.7	0.834	1.112	95.0	0.931	1.201
2	83.3	0.828	1.156	93.3	0.910	1.217
3	86.7	0.785	1.189	91.6	0.899	1.307
4	78.3	0.789	1.394	90.0	0.851	1.667
5	93.3	0.898	1.946	100.0	0.974	2.213

6 Conclusions and Outlooks

We presented an improved version of SURF algorithm that uses descriptor vectors of length 128 based on 8-D descriptor vectors. The important gain in accuracy is due to the use of longer descriptor vectors, which provide more details of images and leads to accurate interest point detection and image registration.

The results showed that the performance of our improved version is comparable and better than the classical one. The high accuracy is advantageous for the cases need high quality of image registration, such as MR infant brain images. As for the commonality of images, the improved SURF algorithm can be used in other different kinds of images, especially color images. Thus, for the future work, in order to widen the application of the improved version, some modifications should be made according to the characteristic of different images.

Although the increase of time consumption is acceptable compared with the accuracy, it is still a drawback for many applications, such as on-line computer vision. Therefore, the reduction of time consumption is an important point for future work.

References

1. Rueekert D, Sonoda L and Hayes C, et al. Nonrigid registration using free-form deformations: application to breast MR images. IEEE Transactions on Medical Imaging, 18(8):712-721, 1999.
2. Zitova B and Flusser J. Image Registration Methods: A Survey. Image and Vision Computing, 21(11):977-1000, 2003.
3. Lisa Gottesfeld Brown. A Survey of Image Registration Techniques. ACM Computing Surveys (CSUR). 24(4):325-376, 1992.
4. Barbara Zitová and Jan Flusser. Image Registration Methods: A Survey. Image and Vision Computing, 21(11):977–1000, 2003.
5. D. G. Lowe. Object recognition from local scale-invariant features. In IEEE International Conference on Computer Vision (ICCV), 1150-1157, Kerkyra, Greece, 1999.
6. D. G. Lowe. Distinctive image features from scale-invariant keypoints, International journal of computer vision, 60(2):91–110, 2004.
7. Bay H, Tuytelaars T and Van Gool L. SURF: Speeded up robust features, Computer Vision–ECCV, 404-417, 2006.
8. Kumar P, Henikoff S, Ng P C. Predicting the effects of coding non-synonymous variants on protein function using the SIFT algorithm, Nature protocols, 4(7):1073-1081, 2009.
9. T. Lindeberg. Scale-space for discrete signals, PAMI, 12(3):234-254, 1990.
10. H Bay, A Ess and T Tuytelaars, et al. Speeded-up robust features (SURF), Computer vision and image understanding, 110(3): 346-359, 2008.
11. T. Lindeberg, Feature detection with automatic scale selection, IJCV 30 (2) 79–116, 1998.
12. Mikolajczyk K, Schmid C. A performance evaluation of local descriptors, IEEE Transactions on Pattern Analysis and Machine Intelligence, 27(10): 1615-1630, 2005.
13. Mikolajczyk K and Schmid C. Scale & affine invariant interest point detectors, International journal of computer vision, 60(1): 63-86, 2004.
14. Zhu Y, Cheng S, Stanković V, et al. Image registration using BP-SIFT, Journal of Visual Communication and Image Representation, 24(4): 448-457, 2013.
15. L.Juan, O.Gwun. Acomparison of SIFT, PCA-SIFT and SURF, Image Process. 3(4)143–152, 2009.
16. Pang Y, Li W, Yuan Y, et al. Fully affine invariant SURF for image matching, Neurocomputing, 85: 6-10, 2012.